Research in Nondestructive Evaluation, 18: 151–161, 2007

ISSN: 0934-9847 print /1432-2110 online
DOI: 10.1080/09349840701305567

Taylor & Francis
Taylor & Francis Group

SOLUTION OF MAXWELL'S EQUATIONS FOR THE SIMULATION AND OPTIMIZATION OF THE RADAR ASSESSMENT OF CONCRETE STRUCTURES

L. Travassos,[1] N. Ida,[2] C. Vollaire,[1] and A. Nicolas[1]

[1]Centre de Genie Electrique Lyon, Lyon, France
[2]University of Akron, Akron, OH, USA

Recent developments in ground-penetrating radar (GPR) models have brought about complex electromagnetic fields due to the fine variations of structures. Therefore, it has become necessary to use more accurate analysis including environmental characteristics, antennas, and interpretation of the raw data in three-dimensional space. Such analyses require numerical techniques by which problems having complex scattering properties can be solved as accurately and as fast as possible. Some methods had been developed for resolution of specific problems involving differential or integral equations. However, each technique has limitations and trade-offs. The research work presented in this article aims to develop electromagnetic wave-propagation models in concrete structures using different numerical techniques to investigate the detection and location of buried objects.

Keywords: FDTD, FEM, GPR, MoM, nondestructive testing

1. INTRODUCTION

Ground-penetrating radar (GPR), or simply radar, is one of the most effective techniques for the detection of inclusions in concrete structures. Over the past decade, this technique has been applied to investigate the integrity of prestressed concrete bridges, tunnels, and roads [1]. It was therefore judged important to pursue the development of forward and inverse numerical analysis to provide the information needed to improve radar assessments.

However, no single numerical method or technique has been found to provide a complete answer in the modeling and optimization of the radar evaluation. For instance, although finite-difference time-domain (FDTD) [2] is well suited for modeling time-dependent scattering, it has difficulty in treating materials with varying properties and discontinuities, which is successfully done by edge finite element (FEM) [3] modeling. The approach in this work is to study the electromagnetic modeling of a radar assessment with various techniques, taking into consideration the problems associated with this evaluation technique. Interpretation and optimization of the radar assessment is also discussed.

Address correspondence to Lucas Travassos, EEA, 36, Guy de Collongue Bat H9, Ecully 69134, France. E-mail: lucas.travassos@ec-lyon.fr

2. NUMERICAL METHODS

For the study and simulation of the electromagnetic (EM) phenomena in any specific application, the solution of Maxwell's equations becomes necessary. EM simulations play an important role in the development of radar testing systems and analysis of data:

- forward scattering is used for analysis of concrete structure configurations,
- inverse scattering is used for imaging of data and classification of detected targets, and
- wave radiation is used for antenna design and optimization.

To model pulsed radar assessment of concrete structures in the reflection mode, the FDTD method was chosen, because of its well-known advantages in modeling transient electromagnetic problems. In this investigation, the goal was to implement efficient algorithms in the time domain for the location of buried targets. Numerical simulations were carried out to show the feasibility of detecting buried pipes using migration algorithms.

In addition, to optimize the field pattern of a bow-tie antenna, a procedure was implemented that unifies multiobjective genetic algorithms and a method of moments [4] (MoM) direct solution with the goal of implementing a tool capable of choosing optimal parameters to achieve the design of an improved GPR antenna. Finally, to simulate more accurately the radar assessment of structures with material discontinuities, FEM was used to complete the investigation.

3. TIME-DOMAIN ANALYSIS

Deterioration and distress mechanisms of the concrete infrastructure are active under the surface and cannot be accurately assessed by visual inspection. Hence, periodic condition assessment of the concrete infrastructure results in better preventive and/or corrective planning, which will preserve its integrity and reduce its life-cycle costs. The radar method is applied as a very effective technique for investigating the integrity of concrete structures thanks to technological advancements over the past decade [1].

However, radar measurements in structures that are only accessible from one side have some limitations, and the method must be optimized to detect a specific target considering the physical characteristics of concrete by selecting the appropriate antenna type, antenna frequency, and antenna configuration. Therefore, the complex design of radar assessment can be aided by using numerical simulation techniques that provide the electromagnetic field behavior when the antenna interacts with a concrete slab.

Three-dimensional FDTD simulations of the assessment of lossless and lossy soils are reported in Refs. [5] and [6], respectively. The influence

of heterogeneity on GPR measurements is examined in Ref. [7]. In this article, we present the methodology and results from three-dimensional (3-D) FDTD modeling of key system aspects relating to the bow-tie antenna-element design, the propagation and scattering of the electromagnetic pulse radiated by this element within a heterogeneous and/or dispersive model of the concrete, and the backscatter response of air/water-filled ducts and buried conductors.

3.1. Summary of Concrete Dielectric Properties

The concrete may be treated as a complex dielectric composed of inorganic material in the dry state with internal free water. The selection of a water/cement (w/c) ratio gives the engineer control over the final properties of the concrete. It is an important decision because it is a trade-off between two desirable properties: strength and workability. The complex permittivity of water changes widely in the frequency bands used in the radar evaluation. Consequently, the mechanical and electric characteristics of the mixture are greatly affected by its water content.

To obtain the dieletric properties of concrete, dielectric models are necessary to determine the effective dielectric properties of a heterogeneous mixture of two or more substances of known permittivities. Factors influencing the effective permittivity of a mixture include the permittivities of the individual substances, their volume fractions, spatial distribution, and shapes of the constituents, and their orientation relative to the electric field vector of the incident electromagnetic waves. To simulate a more realistic concrete model, we use two different approaches:

1. the model proposed by Halabe [8] that deals with complex conductivities instead of complex permittivities and
2. randomly created subsurface heterogeneities.

We performed simulations with two types of concrete; the first is a high-performance concrete and the second is a concrete characterized by bad curing. This high-performance concrete is characterized by a low w/c ratio and use of additives and admixtures together with aggregates to obtain low porosity. Even if the composition is optimal and the compaction is well done, something can go wrong through improper curing, which can determine the concrete's quality. Table 1 shows the properties of the two types of concrete.

According to the discrete grain size model, the permittivities of the two types of concrete can be described using the following Debye parameters, considering the conductivity at the central frequency of 1.5 GHz (Table 2), where, ϵ_∞ is the permittivity at the high-frequency limit and ϵ_s is the static, low-frequency permittivity.

The frequency behavior of the two permittivities is shown in Fig. 1. Considering the simplified depth range (D) and resolution (Δr), Eq. (1)

TABLE 1 Characteristics of Concrete

Parameter	Type 1	Type 2
Degree of saturation	0.2	0.35
Salt content of water (ppm)	60	65
Temperature	20°	20°
Porosity of mixture	0.08	0.2

(with σ in mS/m) and (2), it is more difficult to find any kind of inclusions in concrete structures affected by bad curing because of its higher conductivity (σ) and permittivity (ϵ). The material loss will affect the depth range of the assessment. Using these equations, a transmitted bandwidth (B) of 2.5 GHz, the light speed (c), and targets with a high loss, the depth range for concrete of type 1 and 2 are $D_1 = 1.10$ m and $D_2 = 0.19$ m respectively. The resulting depth resolution is accurate to 2.4 cm for concrete of type 2.

$$D_{max} = \frac{35}{\sigma} \tag{1}$$

$$\Delta r = \frac{c}{2 \cdot B \cdot \sqrt{\epsilon}} \tag{2}$$

Time-domain numerical simulations are performed next to verify the dispersion effects in the detection of buried targets.

3.2. Time-Domain Simulation Results

In the following, we consider a bow-tie antenna shielded with a metal casing. In the FDTD analysis, the slanted edges of the bow-tie antenna are approximated using staircasing with a $\lambda_{cf}/95$ (λ_{cf} is the central frequency wavelength in air) spatial-grid resolution. The transmitting and receiving antennas based on the Geophysical Survey Systems Inc. (GSSI) model described in Ref. [9] are placed side by side immediately above the concrete. The antenna is fed by a 80-Ω transmission line attached to the antenna terminals injecting a differentiated Gaussian voltage pulse with 2.5-GHz bandwidth and central frequency of 1.5 GHz. The targets to be detected are a reinforcement bar and air/water-filled voids and fractures.

Materials having a static conductivity are a serious problem for impedance matched absorbers. Past experience has shown that a classically constructed

TABLE 2 Electrical Characteristics of Concrete

Concrete	ϵ_∞	ϵ_s	$\tau_D(ns)$	σ(S/m)
Type 1	3.857	5.113	0.525	0.031
Type 2	3.981	6.398	0.033	0.182

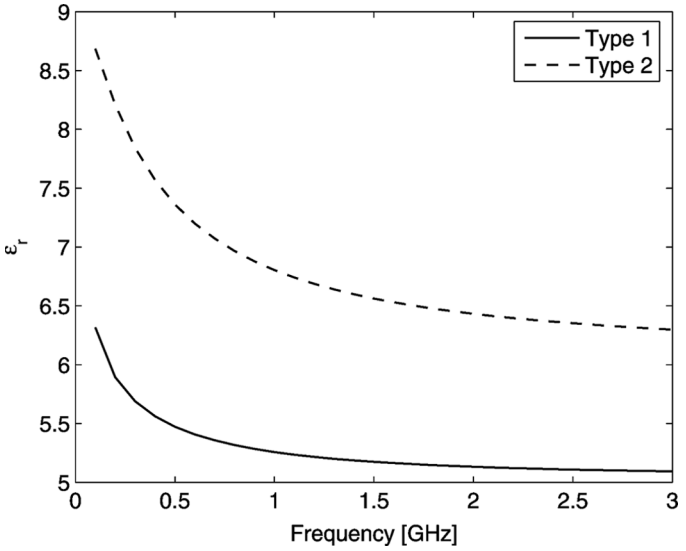

FIGURE 1. Permittivities for concrete of type 1 and 2.

PML (perfectly matched layers) cannot attenuate evanescent modes. Considering the characteristics of the concrete structures analyzed in this work, we used a PML with coordinate stretching [10,11]. Figure 2 shows the FDTD scenario of the simulation. The depth d of the reinforcement bar is 15 cm with radius $r = 1.25$ cm spaced a distance $s = 5$ cm. The simulation was performed with the goal of studying the detection of the reinforcement bars and air- and water-filled fractures in different types of concrete. The 3-D domain used had $150 \times 150 \times 120$ cells with $\Delta = 2.1$ mm and $\Delta t = 4$ ps. Nonorthogonal grid was used to produce a fine mesh in the antenna. Figure 3 shows the reflected signal from different inclusions in concrete of types 1 and 2. In type 1, it is possible to distinguish reflections from different locations. The type 2 concrete

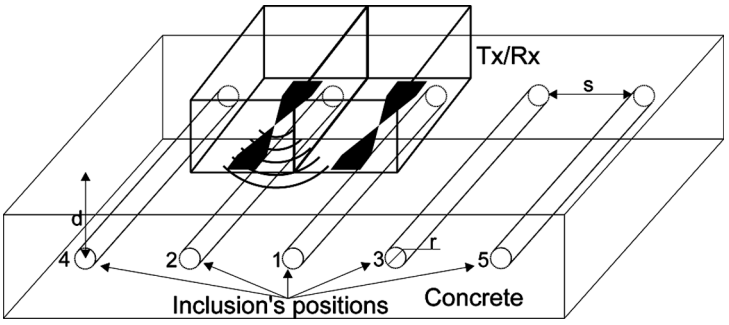

FIGURE 2. FDTD simulation scenario.

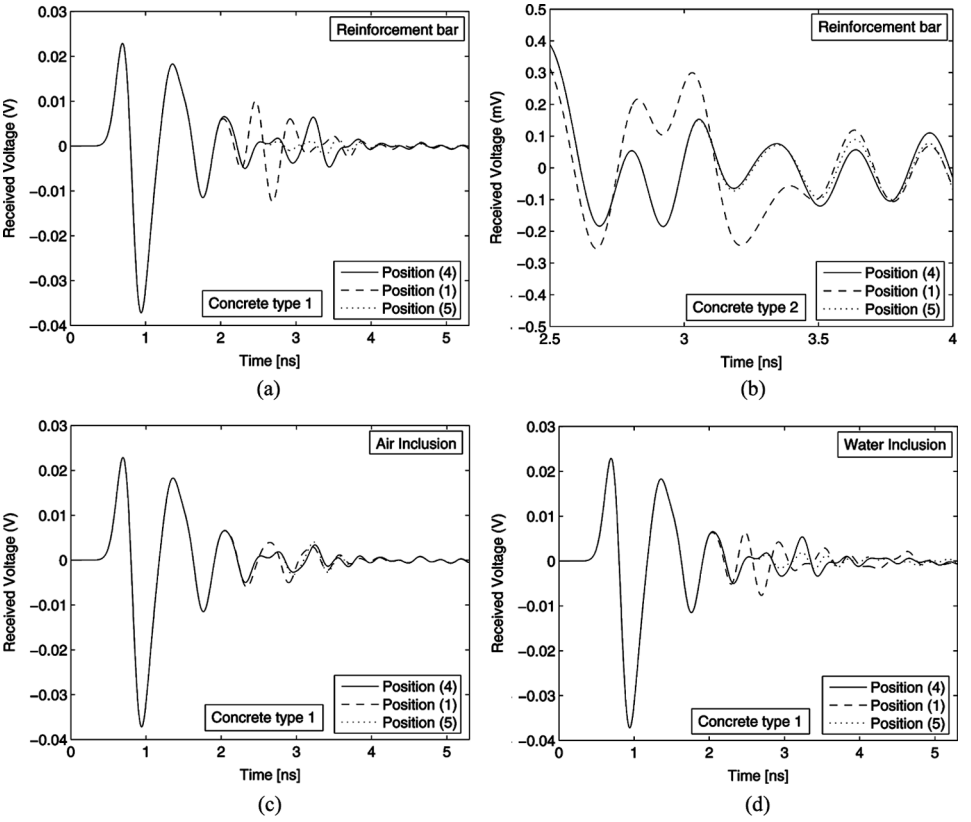

FIGURE 3. Received signal from (a) rebar in type 1 concrete: visual detection in positions (1) and (4); (b) rebar in type 2 concrete: coincident signals; (c) air-filled fracture in type 1 concrete: weak reflected field; (d) water-filled fracture in type 1 concrete: strong reflected field.

produced a reflected wave that normally cannot be detected by measurements. This unexpected result can be explained by the fact that the radar equation does not account for the dispersion effects of the specimen. Figure 3(b) shows that even by applying a time-varying gain in the A-scan, it would be difficult to distinguish between the reflected waves from different target positions. In spite of the relative ease of obtaining the reflected signal from the target, the interpretation of the raw data is a difficult issue. To obtain an improved final image, a migration algorithm was implemented as described in the following sections.

3.3. Migration Algorithm

To improve the interpretation of a radar assessment, a reverse-time migration technique [12] to find the exact location of the targets in heterogeneous media was implemented. The development of this algorithm

is based on the notion of a matched filter, which is used extensively in radar applications. The matched-filter concept can be explained as a correlation of the received signal with the expected or estimated signal from a specific target. If this correlation produces a large value, then it is likely that the target is present. Using this algorithm, an image can be perceived as a back-propagated wave-field reconstruction of the dielectric contrast within the host medium [12]. The final migrated data, $S(\vec{r})$, for a bistatic configuration can be obtained by the following equation:

$$S(\vec{r}) = \sum_{n=1}^{N} \sum_{m=1}^{M} E_{mn,bp}(\vec{r}) \otimes E_{inc}(\vec{r})|_{t=0}, \tag{3}$$

where the subscripts m and n denote the field due to the mth transmitter and nth receiver. Therefore, this expression is interpreted as the intersection (convolution) of the back-propagated field ($E_{mn,bp}$) with the incident field (E_{inc}).

The bistatic algorithm requires propagation of both the incident and back-propagated fields. The data were collected at 60 locations. The final image is created by applying Eq. (4) for the three locations and summing all corresponding results. The implementation in FDTD is accomplished by propagating the incident field in reverse while simultaneously propagating the back-propagated field forward. The FDTD scenario simulated, depicted in Fig. 4(a), consisted of four 12-cm diameter air-filled pipes buried in concrete that was modeled with a mean electrical permittivity value of 6, conductivity of 1 mS/m, and standard deviation of 0.25. Figure 4 shows the FDTD scenario and the final image obtained at $t = 0$ that can be interpreted as the intersection of the back-propagated field with the incident field, providing a more exact location of the hollow tubes.

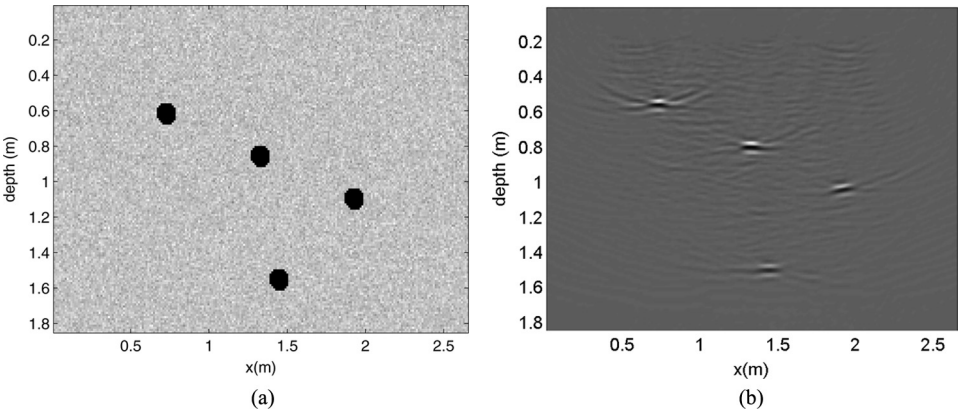

FIGURE 4. Bistatic reverse-time migration: (a) FDTD scenario and (b) final migrated data.

Finally, this process improves the final images provided by the radar inspection data. However, this algorithm assumes that the background medium is known. In addition, in this simulation line sources were used that can create a problem when the objective is to find targets in close proximity. In this case, the antenna used in the assessment should have a narrow beam to detect closely spaced targets. The next section presents a procedure to optimize the field pattern of a bow-tie antenna using multiobjective genetic algorithms in conjunction with a MoM direct solver.

4. ANTENNA OPTIMIZATION

Bow-tie antennas are not isotropic radiators or receivers, and so they exhibit directionality of wavefields. Directivity is an important parameter for imaging applications used to accurately determine the shape, location, and size of subsurface targets and becomes essential when inverting radar data to extract the target's physical properties. The design of an effective planar bow-tie antenna requires balancing the antenna length, the flare angle, and the radiation pattern produced. Therefore, there is a need for optimization in determining the antenna parameters for best performance.

To address the issue of optimization, we considered the problem of where an antenna is in free space and evaluated it in the far-field region. Most antenna characteristics that are relevant to radar applications such as wave polarization, radiation field pattern, and beam width are commonly defined in the far-field region of the antenna. However, notwithstanding the complexity of the electromagnetic radiation in the near-field region, most civil engineering applications using surface contact antennas are concerned with radar measurements in the near-field region [13].

Considering this complexity, FEM is used to investigate the behavior of the optimized antenna in the near-field region of a concrete radar assessment for the location of reinforced bars.

The goal in the optimized design of this antenna is to reduce the metal area (and consequently result in minimal length and weight) and to improve the gain in the plane perpendicular to the antenna. The multiobjective genetic algorithm (MGA) is then coded to find multiple nondominant solutions (the Pareto front) using the method of moments at a fixed frequency of 1 GHz. Details about this procedure can be found in Ref. [14]. The antenna parameters to adjust are

$$P^g = \begin{bmatrix} L^{g,1} & \alpha^{g,1} & E^{g,1} \\ \vdots & \vdots & \vdots \\ L^{g,np} & \alpha^{g,np} & E^{g,np} \end{bmatrix}, \tag{4}$$

where each line represents a feasible solution, g is the current generation, and np is the population size. The variables to be optimized are then the

TABLE 3 Input Data for the MGA Optimization

	Optimization variables		
Limits	Antenna length(λ)	Flare angle (°)	Erased elements (%)
Pareto			
min	0.1	30	0
max	1	120	20
Solution choosen	0.87	79	11

antenna length (L), the flare angle (α), and the percentage of antenna elements (E) that can be removed. They are adjusted to minimize the metal area of the antenna. This becomes the first objective function. The second objective function is to maximize the gain in the direction perpendicular to the antenna plane.

To find the antenna configuration with a higher directivity and a smaller metal area, we implemented an MGA to accomplish two conflicting objectives with the limits shown in Table 3. The solution choosed was the one with a maximal gain in the direction perpendicular to the antenna plane.

First, the antenna is generated with 256 metal elements, and then a percentage of this total between 0 and 20% is replaced with air according to the objectives. The feed region is obviously protected to avoid numerical errors. Figure 5(a) shows the modifications applied to a given solution to improve the radiation pattern.

The radiation pattern depicted in Fig. 5(b) shows the gain obtained in the plane perpendicular to the antenna. The gain obtained was 6.37 dB versus 3.40 dB of a common structure with improvement of the half-power beam width from 57.6° to 43.2°. In this case, the area shown is maximum. Other solutions can be found according to the designer's needs. The convergence

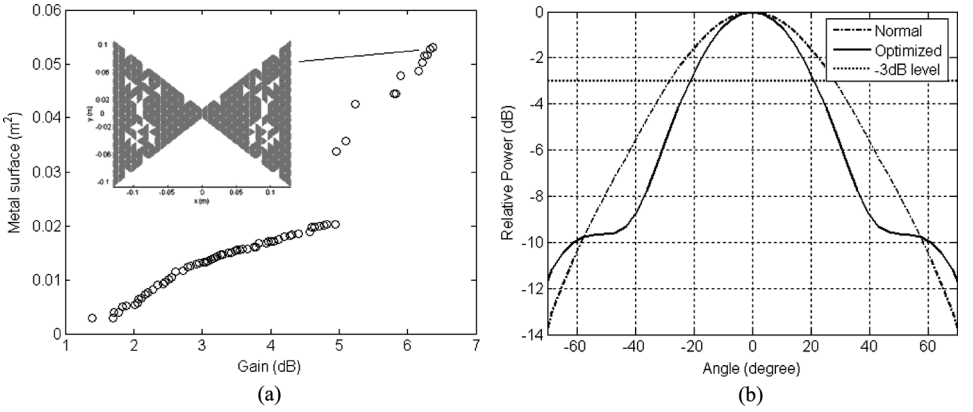

FIGURE 5. Planar bow-tie antenna: (a) pareto-front and optimized antenna, and (b) radiation pattern.

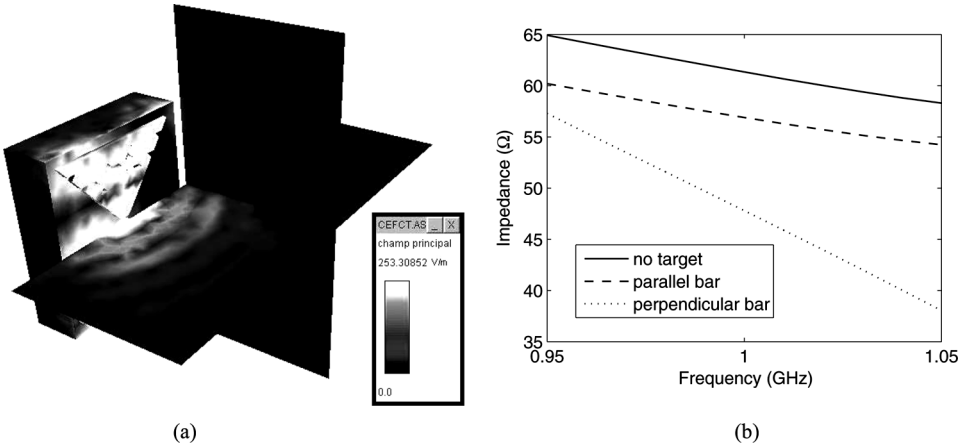

FIGURE 6. Near-field results: (a) FEM simulation and (b) antenna's input impedance.

has been attained in about 50 generations with a population of 50 individuals in several GA executions. The crossover and mutation probabilities were set to 0.9 and 0.05 respectively.

To verify the optimization result, a near field was performed with FEM. The major advantage that FEM has over other EM modeling techniques stems from the fact that this method can model complex geometries and material inhomogeneities accurately. Therefore, FEM was chosen to perform an investigation considering the coupling effects of a geometrically complex antenna over an inhomogeneous dielectric. Moreover, a conductor shield was added to the antenna to improve directivity.

For 1 GHz, the concrete slab was simulated with $\epsilon_r = 8.37$ and $\sigma = 0.23\,\mathrm{S/m}$. First-order boundary conditions were used to truncate the domain of study. The simulation was performed on a Pentium IV with 964 Mb in about 15 min for a domain of 25 K nodes.

The scattered near field shown in Fig. 6(a) illustrates the electric near-field behavior of a nondestructive assessment to detect the presence of a conducting bar buried 15 cm in the concrete and located parallel to the direction of the antenna. Figure 6(b) shows the modifications in the antenna's input impedance for three different scenarios. In the case where the bar is perpendicular to the antenna and consequentially located in the more illuminated region, the input impedance is more strongly affected, indicating its presence.

5. CONCLUSION

Numerical experiments have been performed to analyze different aspects of radar assessment of concrete structures. Results were obtained using various numerical techniques according to the objectives.

Improvements in the interpretation using a reverse-time migration algorithm in conjunction with FDTD has been described. In addition, an algorithm to select the parameters needed to optimize a bow-tie antenna using MoM direct solver and genetic algorithms has been developed. Finally, an FEM investigation was performed to evaluate the feasibility of using this technique to simulate the radar assessment of concrete structures. Performing FEM analysis using an optimized antenna operating above geometrically complex structures will be of interest in forthcoming continued research.

REFERENCES

1. D. J. Daniels. *Ground Penetrating Radar*. Institute of Electrical Engineers, London (2004).
2. A. Taflove and S. Hagness. *Computational Electrodynamics: The Finite-Difference Time-Domain Method*. Artech House, Norwood (2005).
3. P. Monk. *Finite Element Methods for Maxwell's Equations*. Oxford Science Publications, Oxford (2003).
4. R. Bancroft. *Understanding Electromagnetic Scattering using the Moment Method*. Artech House, Boston (1996).
5. D. Uduwawala, M. Norgren, P. Fuks, and A. W. Gunawardena. *IEEE Trans. on Geoscience and Remote Sensing* **51**:732–742 (2004).
6. B. Lampe and K. Holliger. *Geophysics* **70**:K23–K32 (2005).
7. J. J. Holt. *Finite Difference Time Domain Modeling of Dispersion from Heterogeneous Ground Properties in Ground Penetrating Radar*. PhD thesis, Ohio State University, USA (2004).
8. U. B. Halabe. *Condition Assessment of Reinforced Concrete Structures using Electromagnetic Waves*. PhD thesis, Massachusetts Institute of Technology, USA (1990).
9. G. Klysz, J. P. Balayssac, S. Laurens, and X. Ferrieres. *NDT&E International* **39**:338–347 (2006).
10. F. L. Teixeira, Weng Cho Chew, M. Straka, M. L. Oristaglio, and T. Wang. *IEEE Trans. Geoscience and Remote Sensing* **36**:1928–1937 (1998).
11. J. A. Roden and S. D. Gedney. *Microwave Optical Lett.* **27**:334–339 (2000).
12. C. J. Leuschen and R. G. Plumb. *IEEE Trans. Geoscience and Remote Sensing* **3**:295–326 (2001).
13. S. G. Millard, A. Shaari, and J. H. Bungey. *NDT&E International* **35**:473–482 (2002).
14. L. Travassos, S. L. Avila, A. C. Lisboa, C. Vollaire, and A. Nicolas. *The 12th Biennial IEEE Conference on Electromagnetic Field Computation (CEFC 2006)*.